

Recycling of subducted crustal components into carbonatite melts revealed by boron isotopes

Samuel R. W. Hulett¹, Antonio Simonetti^{1*}, E. Troy Rasbury² and N. Gary Hemming³

The global boron geochemical cycle is closely linked to recycling of geologic material via subduction processes that have occurred over billions of years of Earth's history. The origin of carbonatites, unique melts derived from carbon-rich and carbonate-rich regions of the upper mantle, has been linked to a variety of mantle-related processes, including subduction and plume–lithosphere interaction. Here we present boron isotope ($\delta^{11}\text{B}$) compositions for carbonatites from locations worldwide that span a wide range of emplacement ages (between ~ 40 and $\sim 2,600$ Ma). Hence, they provide insight into the temporal evolution of their mantle sources for ~ 2.6 billion years of Earth's history. Boron isotope values are highly variable and range between -8.6‰ and $+5.5\text{‰}$, with all of the young (<300 Ma) carbonatites characterized by more positive $\delta^{11}\text{B}$ values ($>-4.0\text{‰}$), whereas most of the older carbonatite samples record lower B isotope values. Given the $\delta^{11}\text{B}$ value for asthenospheric mantle of $-7 \pm 1\text{‰}$, the B isotope compositions for young carbonatites require the involvement of an enriched (crustal) component. Recycled crustal components may be sampled by carbonatite melts associated with mantle plume activity coincident with major tectonic events, and linked to past episodes of significant subduction associated with supercontinent formation.

Investigations of the boron isotope systematics of a variety of geologic materials have resulted in an increased awareness of the value of this isotope system for geochemical studies, given the number of natural processes that fractionate B isotopes. The large relative mass difference ($\sim 10\%$) between ^{11}B and ^{10}B results in a wide range of B isotope compositions (-30‰ to $+50\text{‰}$) in nature^{1–5}. Moreover, $^{11}\text{B}/^{10}\text{B}$ ratios measured in minerals and whole rocks can be used to trace and model mass transfer processes at subduction zones^{4,5}. The boron-enriched nature of arc-related volcanic rocks (compared with fresh mid-ocean-ridge basalts (MORBs)) has been attributed to the incorporation of boron derived from subducted materials (marine sediments and altered oceanic crust) into the overlying mantle wedge^{4,5}.

To date, the boron isotope systematics of worldwide occurrences of carbonatites (mantle-derived igneous rocks composed of $>50\%$ carbonate minerals) have yet to be investigated. Although they are considered 'exotic' in nature, there are >500 occurrences of carbonatites worldwide and they occur on all continents⁶ (Supplementary Fig. 1). Their predominant CaCO_3 -rich nature implies that carbonatite melt petrogenesis is closely linked to Earth's carbon (C) cycle. Carbon within the mantle may originate from recycling of crustal material by subduction, or it may be primitive, perhaps stored within deeper parts of the mantle. The transfer of C from various mantle sources to carbonate melts is probably intricate, and dependent on the stability of carbonate minerals and in particular on the mantle oxidation state⁷. Due to their unique CaCO_3 -rich composition, carbonatite melts/liquids have a profound effect on the chemical and physical properties of the mantle, such as their influence on partial melting processes⁸, and this in turn controls the distribution/budget of incompatible trace elements and volatiles, rheological and geophysical properties, and metasomatism of the continental lithosphere⁹. Carbonatites range in age from 3.0 billion years ago (Ga) to present day¹⁰, and have thus been used to monitor the secular evolution and degree of chemical heterogeneity

of the upper mantle^{10–12}. The chronological trend of emplacement ages for carbonatite occurrences worldwide, which appears to be spatially and temporally linked to major orogenic cycles, is an increase in carbonatite activity with decreasing geologic age¹³; these features have been attributed to a steady-state process of carbonatite generation and destruction (recycling rate) of ~ 445 million years¹⁴.

Radiogenic (Nd, Sr) isotope investigations of carbonatite complexes from Canada, Russia and Greenland indicate that these regions are characterized by depleted subcontinental mantle that has evolved at relatively constant, time-integrated Rb–Sr and Sm–Nd ratios over billions of years^{10,11} (Fig. 1a). On the basis of experimental results, geochemical results, and Nd, Sr, Pb, C and O isotopic evidence reported thus far¹⁵, it is abundantly clear that carbonatite magmas are mantle-derived. Salient features of radiogenic isotopic (Nd, Sr, Hf, Pb) results from carbonatite complexes worldwide are as follows¹⁵. First, the overlapping isotope ratios measured in young (<200 million years (Myr) old) carbonatites and those for oceanic island basalts (OIBs) indicate derivation from mantle sources (subcontinental mantle and suboceanic mantle, respectively) that are chemically similar in nature; in particular, both require the involvement of HIMU (long-lived high μ (μ represents $^{238}\text{U}/^{204}\text{Pb}$), EMI (enriched mantle I) and FOZO (focal zone) mantle components in the generation of most young (<200 Myr old) carbonatites¹⁶ (Fig. 1b). HIMU and EMI isotope signatures are interpreted to originate from long-lived, subducted oceanic crust and oceanic crust (\pm pelagic sediments), respectively¹⁷; a recent investigation proposes that HIMU represents Archean–early Proterozoic subduction-related carbonatite-metasomatized subcontinental lithospheric mantle that was isolated from convecting mantle for >2.45 billion years, and subsequently entrained and sampled by upwelling plume mantle¹⁸. For young carbonatite complexes from East Africa, it was proposed that both HIMU and EMI components were located within a heterogeneous mantle plume that has been interacting and

¹Department of Civil and Environmental Engineering and Earth Sciences, University of Notre Dame, Notre Dame, Indiana 46556, USA. ²Department of Geosciences, Stony Brook University, New York 11794, USA. ³School of Earth and Environmental Science, Queens College—CUNY, New York 11367, USA. *e-mail: simonetti.3@nd.edu

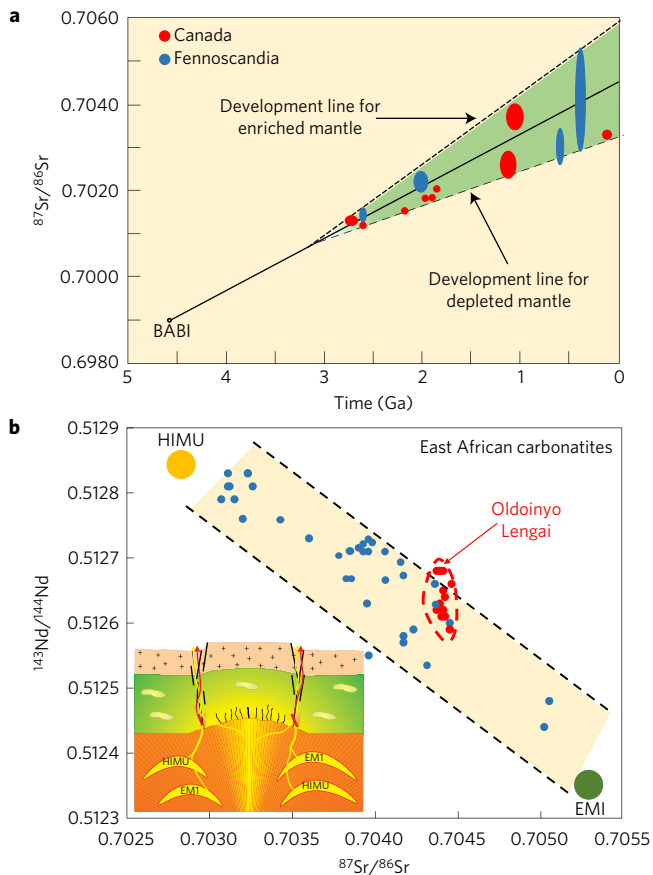


Figure 1 | Nd and Sr isotopic signature of carbonatite magmatism.

a, Illustration displaying initial Sr isotope ratios for carbonatite centres from Canada and Fennoscandia versus emplacement ages. **b**, Diagram illustrating Nd and Sr isotopic data from young (<200 Myr old) East African carbonatite complexes. The data from Oldoinyo Lengai (Tanzania), Earth's only active carbonatite volcano, also plot along the near-linear array between HIMU and EMI. The inset is a schematic cross-sectional view of the upper mantle/crust beneath the East African Rift. Green, subcontinental lithosphere; orange, sublithospheric, isotopically heterogeneous mantle containing pods of HIMU and EMI material (yellow) within a plume upwelling. Figure adapted with permission from ref. 15, Springer.

metasomatizing the overlying lithosphere for the past ~200 million years (Fig. 1b inset)^{15,16}. Second, in contrast, the unradiogenic Hf isotope results for carbonatites and associated alkaline rocks from Greenland indicate generation from an enriched, ancient deep mantle reservoir, possibly representing recycled crustal material¹⁹.

A significant debate continues as to the exact origin of the mantle C giving rise to carbonatite melts over geologic time¹⁵. Carbonatite occurrences worldwide occur predominantly in stable cratonic areas and within continental rifts, but several do occur within or in the vicinity of orogenic belts and oceanic plates⁶. Hence, given this diversity in occurrences, the role of carbonatite magmatism and implications for the mantle C budget on a global scale are important issues to consider. For example, one hypothesis argues that C within carbonatite magmas represents recycled (subducted) carbonate rocks that is subsequently returned to crustal levels by deep mantle plumes^{20–22}. A subduction-related model was also invoked to explain the Neogene to Quaternary magmatic history in Italy, which contains a wide spectrum of rock types including highly alkaline rocks (lamprophyre, lamproite, melilitite, kamaufugites) and carbonatite²². However, HIMU-, EMI- and FOZO-like Sr, Nd and Pb isotope signatures recorded for the highly alkaline rocks are not consistent with a petrogenetic model involving subduction

with eastern migration of a westerly dipping slab, but in contrast were attributed to interaction between several mantle components, namely FOZO and ITEM (Italian enriched mantle) and involved plume-related metasomatic activity²³.

Carbonatites are known to represent crystal cumulates (of predominantly carbonate, with minor silicate and oxide minerals) and not primary melt (liquidus) compositions²⁴. Therefore, interpretations based on isotopic analyses of bulk whole rocks will probably result in a 'mixed' signal due to possible B isotopic fractionation amongst different phases. Hence, to provide an unbiased comparison, this study reports the first comprehensive study of the boron isotope systematics of solely the calcium carbonate (CaCO₃) fraction from 12 occurrences worldwide that range in age from ~40 million years ago (Ma) to ~2,600 Ma (Supplementary Fig. 1). The boron isotopic compositions are used to assess the possible influence of subducted (crustal and sedimentary) components within their mantle source region(s), and provide some temporal constraints on global subduction processes. For example, a recent study argues for the occurrence of subduction and sedimentary input within the mantle as early as 3.5 billion years ago on the basis of nitrogen isotope compositions of kimberlite-hosted diamonds²⁵.

Sample pristinity

Investigating the pristinity (that is, degree of 'freshness') of the carbonatite samples studied here is of utmost importance. However, it may be almost impossible to demonstrate that any suite of magmatic rocks is completely (100%) unaffected by alteration processes. The samples investigated here are inferred to be pristine, unaffected and unaltered by hydrothermal and surficial weathering processes on the basis of several lines of evidence: textural observations obtained via detailed petrographic microscope investigations (Supplementary Figs 2 and 3)²⁶; micro-X-ray fluorescence chemical mapping (Supplementary Fig. 4); stable C and O isotope analyses (Supplementary Table 1 and Fig. 2); and investigating B abundances by *in situ* laser ablation inductively coupled plasma mass spectrometric (LA-ICP-MS) analyses across (core-to-rim) individual carbonate mineral grains (Supplementary Fig. 5). The last of these are challenging to conduct given the very low abundances of boron (<1 ppm) for the samples studied here (Supplementary Table 1), which are essentially at the detection limit of the technique; however, the LA-ICP-MS analyses indicate little or no variation in boron abundances between core and rim areas of individual carbonate grains, and between different mineral phases (that is, calcite versus silicate minerals; Supplementary Fig. 5). With the exception of three samples (Barmer and Amba Dongar, both from India, and Magnet Cove, Arkansas), the B contents for the carbonatites investigated here define a relatively small range of values (~0.04 to ~0.6 ppm; Supplementary Table 1). The B abundances partially overlap those for 'typical' mantle values (<0.1 ppm)^{5,27} and are consistent with those for fresh MORB (<1.5 ppm)²⁵. These low B abundances also preclude interaction (and enrichment) at subsolidus conditions with B-rich crustal materials.

All $\delta^{13}\text{C}$ and $\delta^{18}\text{O}$ values for carbonatite samples investigated here plot within or proximal to the 'primary igneous carbonatite' field²⁸ (Fig. 2), implying that there has been no obvious subsolidus, low-temperature (<500 °C) alteration by hydrothermal or meteoric waters. Such processes would result in dramatic shifts to much heavier C and O isotope values ($\delta^{18}\text{O} > 14\text{‰}$)²⁹ for carbonatites (Fig. 2).

Mixing between mantle sources

B isotope compositions for carbonatites investigated here are listed in Supplementary Table 1, and, importantly, four carbonate sample powders were analysed at two different laboratories (Stony Brook and Notre Dame) with corroborating B isotope results. There are four carbonatite samples characterized by negative $\delta^{11}\text{B}$ values (that is, < -4‰) and these are: Silinjärvi, Finland (2,610 Myr old),

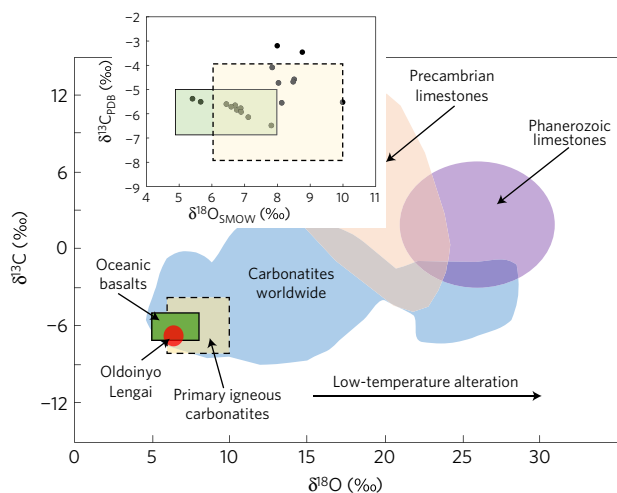


Figure 2 | $\delta^{13}\text{C}_{\text{PDB}}$ (‰) and $\delta^{18}\text{O}_{\text{SMOW}}$ (‰) values for carbonatites worldwide (blue field) compared with those from sedimentary¹⁵ and igneous sources^{28,29}. The inset plots the C and O isotope results obtained for carbonatites investigated here (Supplementary Table 1) and these indicate their pristine nature. Uncertainty or in-run precision (1σ level) associated with an individual data point is within the size of the symbol. Figure adapted with permission from ref. 15, Springer.

Chernigovka, Ukraine (2,090 Myr old), Prairie Lake, Canada (1,170 Myr old), and Kovdor, Russia (370 Myr old; Fig. 3). These $\delta^{11}\text{B}$ compositions (range between -8 and -4 ‰) overlap those for OIBs (-7.6 to -2.1 ‰) from the Azores³⁰, are only slightly higher than the primitive mantle value of -10 ± 2 ‰²⁷, and similar to normal asthenospheric (MORB) mantle ($\sim -7 \pm 1$ ‰)¹. However, it was recently reported³¹ that the highly variable B isotopic compositions of OIB lavas from the Azores are the result of shallow-level assimilation of oceanic crust and not indicative of the presence of subducted material within their mantle source. Combined with their corresponding, typical mantle $\delta^{13}\text{C}$ and $\delta^{18}\text{O}$ ratios (Fig. 2), the negative $\delta^{11}\text{B}$ values (Fig. 3 and Supplementary Table 1) suggest that these carbonatites sampled a mantle source comparable to that of typical MORB mantle. It is unlikely that the low $\delta^{11}\text{B}$ values may be attributed to assimilation of basaltic crust affected by high-temperature hydrothermal alteration²⁷ because carbonatite melts are characterized by low liquidus temperatures (~ 500 to ~ 800 °C)³², and are therefore unlikely to assimilate much basaltic crust. Crustal assimilation will also most likely result in carbonatites characterized by higher $\delta^{13}\text{C}$ and $\delta^{18}\text{O}$ isotope values and with elevated SiO_2 wt% contents. Another possibility is that fenitization (metasomatic alteration) of the country rock, a process attributed to the expulsion of alkali-rich fluids from the differentiating carbonatite melt, may produce B isotope fractionation of the residual carbonatite melt. However, this hypothesis is difficult to evaluate since fenite aureoles are either lacking or not fully developed with all of the carbonatite complexes investigated here (for example, Oka (Québec, Canada), Magnet Cove (Arkansas, US) and Barmer (Rajasthan, India)). Thus, given these considerations, we believe that this issue is difficult to evaluate effectively and is therefore beyond the scope of this study.

The most likely interpretation is that the negative $\delta^{11}\text{B}$ values (< -4 ‰) are inherited from the subcontinental lithospheric mantle, or possibly asthenospheric mantle. The Sr (and Nd to some extent) isotope compositions of carbonatites from Canada, Fennoscandia and Greenland record a range of values, and these are shifted to more radiogenic ratios for each age group^{10,11} (Fig. 1). This has been attributed to mixing and interaction between at least two mantle sources, namely between depleted subcontinental

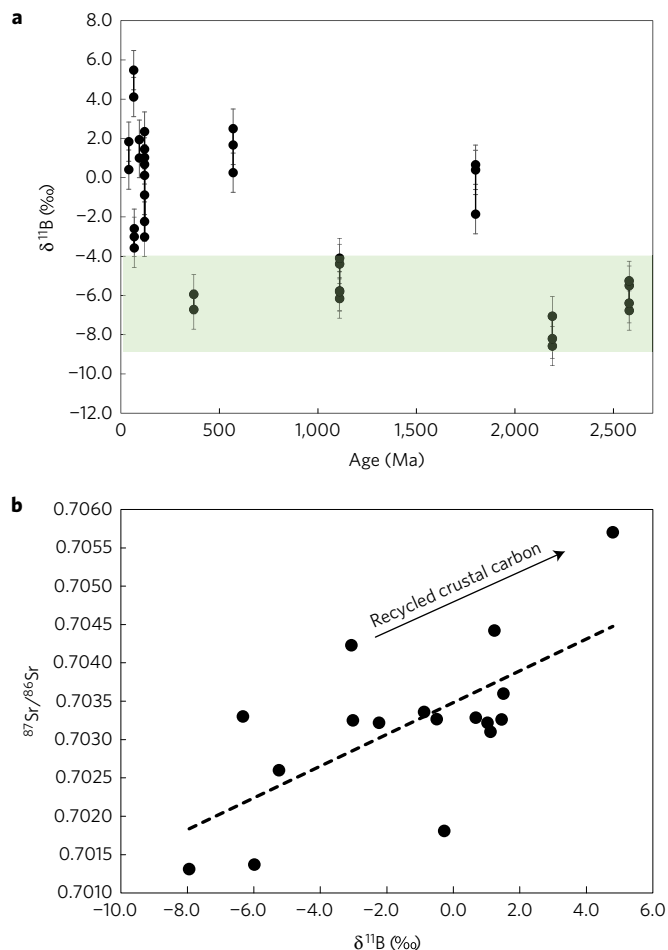


Figure 3 | B isotopic signature of carbonatite magmatism through time. **a**, $\delta^{11}\text{B}$ (‰) values plotted against their respective emplacement ages in millions of years ago (Ma) for worldwide carbonatites. The shaded (green) area is interpreted to represent the B isotopic composition of the depleted subcontinental mantle or MORB-like asthenosphere. The ages for the carbonatites were obtained from various sources^{10,11,33} (Supplementary Table 1). Associated uncertainties are at the 2σ level. **b**, Plot of Sr isotope values^{11,16,33,48–51} against their respective $\delta^{11}\text{B}$ (‰) for carbonatite samples investigated in this study. Average values are plotted for carbonatite complexes reporting multiple whole-rock analyses. The dashed line represents calculated best-fit linear regression.

lithosphere and a more radiogenic endmember originating from the underlying, upwelling (plume) asthenosphere. Plume–lithosphere interaction has been advocated for the generation of carbonatite melts on the basis of their Nd–Pb–Sr isotope systematics (for example, Amba Dongar, India³³). Thus, it is possible that the excursions into more positive $\delta^{11}\text{B}$ values for the complexes of Borden and Iron Hill at $\sim 1,800$ and ~ 570 Myr ago, respectively (Fig. 3) may be attributed to input from an enriched (B isotopic) mantle source, such as an upwelling mantle plume containing more subduction-type material. These more positive values could be related to major orogenic/tectonic events that coincided with increased amounts of crustal material being subducted. Specifically, for Iron Hill this may be related to the suturing of Gondwana, which initiated at ~ 750 Ma and continued until ~ 530 Ma ago³⁴, and for Borden to the assembly of Columbia, a supercontinent that formed between ~ 2.0 and ~ 1.8 billion years ago³⁵.

Thermodynamic–geochemical modelling and data indicate that fluids expelled during dehydration of subducting oceanic crust exhibit decreasing $\delta^{11}\text{B}$ values (from $> +10$ ‰ to ~ -10 ‰) with

increasing depth^{4,36}, and with continued subduction and at deeper mantle levels between ~175 and ~225 km, serpentine dehydration within the underlying mantle slab (oceanic lithosphere) produces fluids characterized by positive $\delta^{11}\text{B}$ compositions ($>0\%$) when water contents of the slab mantle are $>2.5\text{ wt}\%$ (ref. 4). Importantly, involvement of subducted crustal material in mantle carbonate melt formation is evidenced from the Sr, Nd and Pb isotope signatures of young ($<200\text{ Myr}$ old) carbonatites worldwide, which indicate the mixing of HIMU and EMI mantle components¹⁶ (Fig. 1). For example, Fig. 3 illustrates the overall positive correlation between the Sr isotope ratios and $\delta^{11}\text{B}$ compositions for the carbonatites investigated here, and provides evidence that the higher $^{87}\text{Sr}/^{86}\text{Sr}$ values are not the result of simple, closed system, time-integrated radiogenic in-growth of ^{87}Sr due to the decay of ^{87}Rb . As shown in Fig. 1, it is clear that a depleted mantle component (time-integrated Rb/Sr lower than bulk Earth ~ 0.03) is involved in the generation of carbonatite complexes worldwide. However, the $\delta^{11}\text{B}$ compositions reported in this study greater than that of typical asthenospheric mantle (-7%)¹ indicate that the radiogenic component must be related to an endmember characterized by a heavier B isotopic composition, such as recycled crustal material. To date, one of the main arguments against the involvement of subducted crustal material within the mantle source region giving rise to carbonatite melts is the marked absence of carbonatitic activity in the vicinity of present-day subduction zones¹⁵. However, this argument assumes that any carbonate (or C-bearing phase) associated with the subducted material will have a short residence time in the mantle and be recycled back to arc volcanism and not survive to deeper, lower mantle levels. On the basis of experimental data, there is some debate as to the vertical extent of the deep carbon cycle within the mantle since arguments restrict it to $<300\text{ km}$ depth³⁷, or to much deeper levels^{38,39}. As recently summarized and discussed⁴⁰, the presence of both higher geothermal gradients and mantle convection rates until ~ 1.5 billion years ago resulted in variable subduction rates that reduced the likelihood of adding crustal carbon into the deep mantle. As Earth's mantle cooled, the global C cycle may have changed by the Meso- to Neoproterozoic (between ~ 1.6 to ~ 0.5 billion years ago)⁴⁰. During the latter, the mantle environment of subduction zones most likely permitted influx of crustal-derived carbonates beyond the depth of arc-magma generation, which resulted in the more efficient addition of C into the deep mantle⁴⁰. If indeed subducted materials are transported past the mantle transition zone, then it is probable that C subducted during the Proterozoic and Phanerozoic periods may have accumulated in the deep mantle⁴⁰. Thus, with the increased efficiency to process and accumulate crustal C in the deep mantle with decreasing geologic age, then long-term storage and extraction mechanisms become vital factors in controlling the global C budget⁴⁰. As previously discussed⁴¹, it is possible that thermal anomalies within the deep mantle and at the core–mantle boundary result in the production of plumes, and consequently these may be efficient transport vehicles in bringing older, subducted crustal carbon to the surface. Hence, carbon contained within carbonatites associated with plume activity may have originated from old, crustal sources.

Recent ($<300\text{ Myr}$) mantle geodynamics

Carbonatites $<300\text{ Myr}$ old define the most extreme variations in both B contents (range between 0.06 and 2.1 ppm; Supplementary Table 1) and $\delta^{11}\text{B}$ compositions (between -3.58% and $+5.48\%$; Fig. 2). Both features suggest a major change in the mantle geodynamic conditions giving rise to these carbonatites. One possible major geotectonic event that could have changed conditions in the upper mantle is the coalescence ($\sim 300\text{ Ma}$) and subsequent breakup ($\sim 175\text{ Ma}$) of the Pangaea supercontinent⁴². Alternatively, several hypotheses advocate for differing start times

for the onset of the modern style of subduction tectonics, one being that it began in the Neoproterozoic⁴³. If indeed the case, then these combined events may have exerted significant effects on deep mantle convection, which may have resulted in a greater amount of subducted material being brought up by subsequent plume activity³⁶. Seismic tomographic results indicate that subducted mantle slabs penetrate deep into the lowermost mantle and possibly to the core–mantle boundary⁴⁴, which may be a location of plume production⁴¹. As discussed earlier, previous radiogenic isotope studies have advocated for the link between carbonatites and mantle plumes; the association of the latter with the production of large igneous provinces⁴⁵ opens the possibility that greater plume production commenced within the last ~ 300 to ~ 400 million years, and with it more associated carbonatite occurrences characterized by variable and higher $\delta^{11}\text{B}$ compositions.

The formation of the Pangaea supercontinent and/or the change to modern style of subduction tectonics in the Neoproterozoic may have provided the necessary mantle turnover to overprint the prevalent B isotopic composition of the mantle. Given the age distribution and B isotope data at hand, it is difficult to evaluate the impacts of the formation and destruction of older supercontinents, such as Gondwana and Rodinia. As stated earlier, the global terrestrial C cycle was not constant throughout Earth's geologic history⁴⁰, with shallower-level carbonate-generated partial melting and C outgassing being more prevalent prior to the Meso- and Neoproterozoic due to higher mantle geothermal gradients and convection rates. The positive $\delta^{11}\text{B}$ compositions (0 to $\sim 2.5\%$; Fig. 3) recorded by the Iron Hill carbonatite may reflect plate tectonic activity associated with formation of the Gondwana supercontinent, but this is only one complex and further investigation into this hypothesis is needed. By proxy, the source of subducted C may have changed dramatically to more biogenic in nature with the 'Cambrian Explosion' event that occurred ~ 550 million years ago⁴⁶. Corroborating evidence is shown in Supplementary Fig. 6 as a steady (overall) increase in the $\delta^{11}\text{B}$ values (from ~ 6 to $\sim 22\%$) is recorded for marine carbonates globally from the Ordovician/Silurian to present day. Moreover, the overall global increase in the $^{87}\text{Sr}/^{86}\text{Sr}$ ratios of marine carbonates with decreasing geologic time⁴⁷ will result in C characterized by more radiogenic Sr being recycled into the mantle, and is consistent with the positive correlation between Sr and B isotope values (Fig. 3). Additional work is needed in reporting the B isotope compositions of carbonatite complexes worldwide, and combining these results with both their radiogenic and stable isotope values will help to improve our understanding of the terrestrial carbon cycle throughout Earth history.

Methods

Methods, including statements of data availability and any associated accession codes and references, are available in the [online version of this paper](#).

Received 17 June 2016; accepted 3 October 2016;
published online 7 November 2016

References

1. Chaussidon, M. & Jambon, A. Boron content and isotopic composition of oceanic basalts: geochemical and cosmochemical implications. *Earth Planet. Sci. Lett.* **259**, 541–556 (1994).
2. Spivack, A. J. & Edmond, J. M. Boron isotope exchange between seawater and the oceanic crust. *Geochim. Cosmochim. Acta* **51**, 1033–1043 (1987).
3. Palmer, M. R. & Swihart, G. H. Boron isotope geochemistry: an overview. *Rev. Mineral.* **33**, 709–744 (1996).
4. Konrad-Schmolke, M. & Halama, R. Combined thermodynamic-geochemical modeling in metamorphic geology: boron as tracer of fluid-rock interaction. *Lithos* **208–209**, 393–414 (2014).
5. Wunder, B., Meixner, A., Romer, R. L., Wirth, R. & Heinrich, W. The geochemical cycle of boron: constraints from boron isotope partitioning experiments between mica and fluid. *Lithos* **84**, 206–216 (2005).

6. Woolley, A. R. & Kjarsgaard, B. A. *Carbonatite Occurrences of the World: Map and Database* (Geological Survey of Canada, 2008).
7. Luth, R. W. Diamonds, eclogites, and the oxidation-state of the Earth's mantle. *Science* **261**, 66–68 (1993).
8. Dasgupta, R. & Hirschmann, M. M. Melting in the Earth's deep upper mantle caused by carbon dioxide. *Nature* **440**, 659–662 (2006).
9. Yaxley, G. M., Green, D. H. & Kamenetsky, V. Carbonatite metasomatism in the southeastern Australian lithosphere. *J. Petrol.* **39**, 1917–1930 (1998).
10. Rukhlov, A. S. & Bell, K. Geochronology of carbonatites from the Canadian and Baltic Shields, and the Canadian Cordillera: clues to mantle evolution. *Mineral. Petrol.* **98**, 11–54 (2010).
11. Bell, K., Blenkinsop, J., Cole, T. J. S. & Menagh, D. P. Evidence from Sr isotopes for long-lived heterogeneities in the upper mantle. *Nature* **298**, 251–253 (1982).
12. Halama, R., McDonough, W. F., Rudnick, R. L. & Bell, K. Tracking the lithium isotopic evolution of the mantle using carbonatites. *Earth Planet. Sci. Lett.* **265**, 726–742 (2008).
13. Woolley, A. R. *The Spatial and Temporal Distribution of Carbonatites: Carbonatites: Genesis and Evolution* Ch. 2 (Unwin Hyman, 1989).
14. Veizer, J., Bell, K. & Jansen, S. L. Temporal distribution of carbonatites. *Geology* **20**, 1147–1149 (1992).
15. Bell, K. & Simonetti, A. Source of parental melts to carbonatites—critical isotopic constraints. *Mineral. Petrol.* **98**, 77–89 (2010).
16. Bell, K. & Tilton, G. R. Probing the mantle: the story from carbonatites. *Eos Trans. Am. Geophys. Union* **83**, 273–280 (2002).
17. Zindler, A. & Hart, S. R. Chemical dynamics. *Annu. Rev. Earth Planet. Sci.* **14**, 493–571 (1986).
18. Weiss, Y., Class, C., Goldstein, S. L. & Hanyu, T. Key new pieces of the HIMU puzzle from olivines and diamond inclusions. *Nature* **537**, 666–670 (2016).
19. Bizzarro, M., Simonetti, A., Stevenson, R. K. & David, J. Hf isotope evidence for a hidden mantle reservoir. *Geology* **30**, 771–774 (2002).
20. Barker, D. S. Consequences of recycled carbon in carbonatites. *Can. Mineral.* **34**, 373–387 (1996).
21. Hoernle, K., Tilton, G., Le Bas, M. J., Duggen, S. & Garbe-Schönberg, D. Geochemistry of oceanic carbonatites compared with continental carbonatites: mantle recycling of oceanic crustal carbonate. *Contrib. Mineral. Petrol.* **142**, 520–542 (2002).
22. D'Orazio, M., Innocenti, F., Tonarini, S. & Doglioni, C. Carbonatites in a subduction system: the Pleistocene alkivites from Mt. Vulture (southern Italy). *Lithos* **98**, 313–334 (2007).
23. Bell, K., Lavecchia, G. & Rosatelli, G. Cenozoic Italian magmatism—Isotope constraints for possible plume-related activity. *J. South Am. Earth Sci.* **41**, 22–40 (2013).
24. Mitchell, R. H. Carbonatites and carbonatites and carbonatites. *Can. Mineral.* **43**, 2049–2068 (2005).
25. Smart, K. A., Tappe, S., Stern, R. A., Webb, S. J. & Ashwal, L. D. Early Archaean tectonics and mantle redox recorded in Witwatersrand diamonds. *Nat. Geosci.* **9**, 255–259 (2016).
26. Hulett, S. W. R. *Boron Abundances and Isotope Systematics of Carbonatites from Worldwide Sources* MS thesis, Univ. Notre Dame (2016).
27. Chaussidon, M. & Marty, B. Primitive boron isotope composition of the mantle. *Science* **269**, 383–386 (1995).
28. Keller, J. & Hoefs, J. *Stable Isotope Characteristics of Recent Natrocarbonatites from Oldoinyo Lengai: Carbonatite Volcanism IAVCEI Proceedings in Volcanology* Vol. 4 (Springer, 1995).
29. Deines, P. *Stable Isotope Variations in Carbonatites: Carbonatites: Genesis and Evolution* Ch. 13 (Unwin Hyman, 1989).
30. Turner, S., Tonarini, S., Bindeman, I., Leeman, W. P. & Schaefer, B. F. Boron and oxygen isotope evidence for recycling of subducted components over the past 2.5 Gyr. *Nature* **447**, 702–705 (2007).
31. Genske, F. S. *et al.* Lithium and boron isotope systematics in lavas from the Azores islands reveal crustal assimilation. *Chem. Geol.* **273**, 27–36 (2014).
32. Jones, A. P., Genge, M. & Carmody, L. Carbonate melts and carbonatites. *Rev. Mineral. Geochem.* **75**, 289–322 (2013).
33. Simonetti, A., Goldstein, S. L., Schmidberger, S. S. & Viladkar, S. G. Geochemical and Nd, Pb, and Sr isotope data from Deccan alkaline complexes—Inferences for mantle sources and plume–lithosphere interaction. *J. Petrol.* **39**, 1847–1864 (1998).
34. Meert, J. G. A synopsis of events related to the assembly of eastern Gondwana. *Tectonophysics* **362**, 1–40 (2003).
35. Zhao, G., Sun, M., Wilde, S. A. & Li, S. Assembly, accretion and breakup of the Paleo-Mesoproterozoic Columbia Supercontinent: records in the North China Craton. *Gondwana Res.* **6**, 417–434 (2003).
36. Shaw, A. M. *et al.* Long-term preservation of slab signatures in the mantle inferred from hydrogen isotopes. *Nat. Geosci.* **5**, 224–228 (2012).
37. Hammouda, T. High-pressure melting of carbonated eclogite and experimental constraints on carbon recycling and storage in the mantle. *Earth Planet. Sci. Lett.* **214**, 357–368 (2003).
38. Yaxley, G. M. & Brey, G. P. Phase relations of carbonate-bearing eclogite assemblages from 2.5 to 5.5 GPa: implications for petrogenesis of carbonatites. *Contrib. Mineral. Petrol.* **146**, 606–619 (2004).
39. Dasgupta, R., Hirschmann, M. M. & Withers, A. W. Deep global cycling of carbon constrained by the solidus of anhydrous, carbonated eclogite. *Earth Planet. Sci. Lett.* **227**, 73–85 (2004).
40. Dasgupta, R. Ingressing, storage, and outgassing of terrestrial carbon through geologic time. *Rev. Mineral. Geochem.* **75**, 183–229 (2013).
41. Lay, T., Hernlund, J. & Buffett, B. A. Core-mantle boundary heat flow. *Nat. Geosci.* **1**, 25–32 (2008).
42. Collins, W. J. Slab pull, mantle convection, and Pangaea assembly and dispersal. *Earth Planet. Sci. Lett.* **205**, 225–237 (2003).
43. Stern, R. J. Evidence from ophiolites, blueschists, and ultrahigh-pressure metamorphic terranes that the modern episode of subduction tectonics began in Neoproterozoic time. *Geology* **33**, 557–560 (2005).
44. van der Hilst, R. D., Widiyantoro, S. & Engdahl, E. R. Evidence for deep mantle circulation from global tomography. *Nature* **386**, 578–584 (1997).
45. Ernst, R. E. & Bell, K. Large igneous provinces (LIPs) and carbonatites. *Mineral. Petrol.* **98**, 55–76 (2010).
46. Maloof, A. C. *et al.* The earliest Cambrian record of animals and ocean geochemical change. *Geol. Soc. Am. Bull.* **122**, 1731–1774 (2010).
47. Mirota, M. D. & Veizer, J. Geochemistry of Precambrian carbonates: VI. Apehian Alabell Formations, Quebec, Canada. *Geochim. Cosmochim. Acta* **58**, 1735–1745 (1994).
48. Bell, K. & Blenkinsop, J. *Neodymium and Strontium Isotope Geochemistry of Carbonatites: Carbonatites: Genesis and Evolution* Ch. 12 (Unwin Hyman, 1989).
49. Bell, K. & Tilton, G. R. Nd, Pb and Sr isotope compositions of East African carbonatites: evidence for mantle mixing and plume inhomogeneity. *J. Petrol.* **42**, 1927–1945 (2001).
50. Zagnitko, V., Kryvdik, S. & Donskiy, M. Isotope geochemistry of carbonatites of Ukraine. *Period. Mineral.* **72**, 153–159 (2003).
51. Chen, W. & Simonetti, A. Isotopic (Pb, Sr, Nd, C, O) evidence for plume-related sampling of an ancient, depleted mantle reservoir. *Lithos* **216–217**, 81–92 (2015).

Acknowledgements

We thank K. Bell for donating most of the carbonatite samples investigated here. S. Hulett is appreciative of the assistance provided by D. Birdsell (Center for Environmental Science Technology (CEST), University of Notre Dame) in relation to the stable C and O isotope analyses and use of the micro-X-ray fluorescence instrument. I. Steele and B. Monaco are thanked for help with conducting EMP and LA-ICP-MS analyses. The work reported here was possible owing to financial support from the University of Notre Dame.

Author contributions

A.S. and S.R.W.H. conceived the model and prepared the initial manuscript. S.R.W.H. conducted all of the analytical work reported here at the University of Notre Dame, and E.T.R. and N.G.H. supervised S.R.W.H. during a 1-week instructional visit at Stony Brook. E.T.R. conducted the ion exchange chemistry and B isotope analyses on four carbonatite samples at Stony Brook University. All authors contributed to preparation of the final manuscript.

Additional information

Supplementary information is available in the [online version of the paper](#). Reprints and permissions information is available online at www.nature.com/reprints. Correspondence and requests for materials should be addressed to A.S.

Competing financial interests

The authors declare no competing financial interests.

Methods

Sample preparation and boron chemistry, University of Notre Dame.

Carbonatite samples are from locations worldwide (Supplementary Fig. 1). Doubly-polished thin sections were produced from representative pieces of carbonatite samples investigated here, and these were examined in detail using a petrographic microscope (Supplementary Figs 2 and 3)²⁶. Qualitative major element chemical mapping was conducted using an EDAX Orbis micro energy dispersive X-ray fluorescence instrument (for example, Supplementary Fig. 4).

All reagents employed were monitored for their background levels of boron. Laboratory and hood blanks were ascertained by leaving empty Savillex vials open for 97 h. Laboratory and reagent blanks are reported in Supplementary Table 2. All recorded B laboratory blanks for the various Notre Dame laboratories are lower than the average value of 4 pg h^{-1} reported in a recent study⁵². Handpicked separates were powdered by mortar and pestle and then digested in 15 ml Savillex Teflon beakers using double-distilled HNO_3 . Due to the low B content (0.1–1 ppm) in most carbonatite samples, the amount of sample processed ranged from 0.05 g to 1 g. Samples were then dried down and subsequently re-dissolved with 2% HNO_3 , and then buffered to a pH of 5 using a 20% Na acetate solution. At this pH, Amberlite IRA-743 resin has a partition coefficient for boron of $\sim 10^4$, which was used for separation of B from the calcite matrix⁵³.

Stony Brook analytical techniques. On the basis of boron concentrations (Supplementary Table 1), samples were weighed into 7 ml vials to achieve at least 25 ng of boron, and then dissolved in 8 N high-purity nitric acid (Aristar). After dissolution, the samples were dried down and then re-dissolved in 2 N nitric acid. The solutions were centrifuged to remove insoluble residue and then adjusted to a pH of ~ 8 using full-strength Seastar ammonia solution. The ion exchange micro-column chemistry was conducted using boron-specific resin, with the elution flow rate controlled via a peristaltic pump, which is the identical technique used at Notre Dame. Mannitol was added to the boron (in a 1:1 molar ratio) to prevent volatilization. The total procedural blank is between 0.2–0.7 ng. Samples were run on a Nu Plasma II MC ICPMS at Stony Brook using the same configuration and data acquisition as that at Notre Dame. Mannitol is added to the NBS 951 standard for matrix matching to the samples. The running average for the $\delta^{11}\text{B}$ value of the NIST SRM 951a standard processed through the B ion exchange chemistry and mass spectrometry is $0.02 \pm 0.8\text{‰}$ (2σ level).

Boron concentrations. Boron abundances of calcite separates were obtained via solution-mode, high-resolution inductively coupled plasma mass spectrometry. A certified boron elemental standard solution was used for an external calibration protocol, and ^{75}As was employed as an internal standard to monitor and correct for instrumental drift using a sample-standard bracketing technique. Determination of elemental abundances, detection limits, and internal uncertainties were calculated using Excel-based spreadsheets for the Oka samples, and with both Excel worksheets and the NuQuant data reduction software (Nu Instruments) for the remaining samples.

B isotope ratio determinations by MC-ICP-MS. B aliquots were analysed in solution mode using a Nu Plasma II multi-collector ICP-MS. For each analytical session, instrument tuning was conducted using a 100 ppb solution of the NIST SRM 951a boric acid standard. Instrumental drift was corrected by using a sample-standard bracketing technique involving a 100 ppb NIST SRM 951a boron isotope standard solution in 2% HNO_3 . All samples were analysed at a concentration of ~ 100 – 120 ppb, which yielded between 0.7 V and 1.2 V of total B ion signal, and therefore results are reported as delta values without further normalization. The introduction system employed was devoid of borosilicate glass since it consisted of a PFA spray chamber encased in a Peltier cooling device set to 7°C , and a demountable quartz torch equipped with a sapphire injector. Each analysis consisted of a 2 min 'on-peak' zero cycle followed by a single 2 min analysis cycle consisting of simultaneous measurement of ^{10}B and ^{11}B ion signals on Faraday collectors L6 and H7, respectively. Duplicate and triplicate analyses of carbonatite sample powders were not necessarily processed and measured during the same analytical session. Reproducibility was determined by repeated analysis of the 100 ppb NIST SRM 951a B isotopic standard and then determined using the equation: $\sigma \{a_1, a_2, \dots\} \times 2\bar{x} \{a_1, a_2, \dots\} \times 100$, where a represents analysis of the standard, and typically ranged between 0.5 and 1.0‰ (2σ level) for each analytical session.

$\delta^{13}\text{C}$ and $\delta^{18}\text{O}$ compositions. Carbon and oxygen isotope analyses of calcite were conducted using the conventional orthophosphoric acid digestion method⁵⁴. Carbon and oxygen isotope data are reported in per mil notation (‰) using standard δ notation as $\delta^{13}\text{C}$ and $\delta^{18}\text{O}$ values relative to standard mean ocean water (SMOW)⁵⁵ and PeeDee belemnite (PDB)⁵⁶, respectively. Analysis of standard NBS 19 yielded C and O isotopic ratios identical to certified values ($\delta^{13}\text{C} = 1.95\text{‰}$, $\delta^{18}\text{O} = 28.65\text{‰}$)⁵⁴.

Data availability. The authors declare that the data supporting the findings of this study are available within this article and its Supplementary Information files.

References

- Foster, G. L. Seawater pH, pCO_2 and $[\text{CO}_3^{2-}]$ variations in the Caribbean Sea over the last 130 kyr: a boron isotope and B/Ca study of planktic foraminifera. *Earth Planet. Sci. Lett.* **271**, 254–266 (2008).
- Lemarchand, D., Gaillardet, J., Göpel, C. & Manhès, G. An optimized procedure for boron separation and mass spectrometry analysis for river samples. *Chem. Geol.* **182**, 323–334 (2002).
- McCrea, J. M. On the isotopic chemistry of carbonates and a paleotemperature scale. *J. Chem. Phys.* **18**, 849–857 (1950).
- Coplen, T. B. *et al.* New guidelines for $\delta^{13}\text{C}$ measurements. *Anal. Chem.* **78**, 2439–2441 (2006).
- Craig, H. Standard for reporting concentrations of deuterium and oxygen-18 in natural waters. *Science* **133**, 1833–1834 (1961).